Biogeochemistry (2008) 91:133–150
DOI 10.1007/s10533-008-9265-9

Riparian zone denitrification affects nitrogen flux through a tidal freshwater river

Scott H. Ensign · Michael F. Piehler · Martin W. Doyle

Received: 4 July 2008 / Accepted: 7 November 2008 / Published online: 3 December 2008

Abstract Tidal freshwater zones (TFZ) of coastal rivers link terrestrial watersheds to the ocean and are characterized by large, regularly inundated riparian zones. We investigated the effect of riparian denitrification on nitrogen flux in the TFZ Newport River, North Carolina (U.S.A.) by developing an empirical model of denitrification and parameterizing it using measured denitrification rates, sediment oxidation-reduction potential dynamics, and riparian topography. Denitrification rates were measured monthly in laboratory-incubated sediment cores by using a membrane inlet mass spectrometer to assess net water-borne N_2 flux from the cores. Annual average rates of denitrification in three intertidal riparian habitats, emergent marsh, mudflat, and hardwood forest, were 1864, 1956, and 2018 $\mu g\ m^{-2}\ h^{-1}$, respectively. Laboratory experiments and in-situ monitoring revealed that the temporal lag between tidal inundation and reduced, denitrifying conditions was 4–5 h. Field measurements and remotely sensed data showed that the inundated surface area during high tide was three times greater than that at low tide. By combining data on denitrification, oxidation-reduction potential, and topography, the model predicted that the daily denitrification flux constituted 2–15% of the daily riverine nitrate flux during most of the year and >100% during low discharge periods. Current regional and global nitrogen budgets thus may overestimate nitrogen delivery to the ocean by not accounting for the TFZ denitrification.

Keywords Denitrification · Tidal freshwater zone · Riparian floodplain · River nitrogen budget

Abbreviations

TFZ	Tidal freshwater zone
UNC-IMS	University of North Carolina Institute of Marine Sciences
LIDAR	Light image detection And ranging
TIN	Triangulated irregular network

S. H. Ensign
Curriculum in Ecology, University of North Carolina at Chapel Hill, Chapel Hill, NC, USA

S. H. Ensign (✉) · M. F. Piehler
Institute of Marine Sciences, University of North Carolina at Chapel Hill, 3431 Arendell Street, Morehead City 28557, USA
e-mail: ensign@email.unc.edu

M. W. Doyle
Department of Geography, University of North Carolina at Chapel Hill, Chapel Hill, NC, USA

Introduction

Along the hydrologic continuum between streams and oceans lies a unique ecotone where river meets estuary. In this tidal freshwater zone (TFZ) river flow is tidally-influenced but is upstream of saltwater intrusion. This hydrologic variability affects river

geomorphology, river discharge, and biogeochemistry, making the TFZ ecologically distinct from non-tidal rivers (Schuchardt et al. 1993). These differences between tidal and non-tidal rivers pose a challenge to watershed-scale biogeochemical research for two reasons. First, measurement of downstream elemental flux in TFZ rivers is obscured by constantly changing discharge over hourly timescales due to varying water level and velocity. Consequently, riverine fluxes of environmentally important elements are commonly measured upstream of the TFZ, thereby omitting a sizable portion of the lower watershed (Destouni et al. 2008). Second, the unique geomorphology and hydrology of the TFZ make it difficult to apply riverine biogeochemical models to this portion of the river continuum. Fundamental information on how TFZ geomorphology and hydrology influence biogeochemical processes is needed to properly include this ecotone in river and watershed elemental budgets.

Nitrogen budgets for watersheds, regions, and the globe are continually being refined due to the importance of this element for biological production and also because of its role as a pollutant that has caused environmental degradation of freshwater and marine ecosystems (Vitousek et al. 1997; Smith et al. 1999; Green et al. 2004). River networks and associated lakes and reservoirs are highly reactive with respect to nitrogen and remove 53% of their terrestrially-derived nitrogen load prior to reaching the oceans (Wollheim et al. 2008), principally through the microbially-mediated process of denitrification (Seitzinger et al. 2006). However, regional and global models of riverine nitrogen attenuation (See Boyer et al. 2006; Wollheim et al. 2006 for review) have not accounted for TFZ biogeochemistry differently from the rest of the river network, and it is unknown what affect this may have on model accuracy.

One unique characteristic of the TFZ that may have a large effect on riverine nitrogen flux is their expansive riparian floodplains. Denitrification in floodplain soils can substantially decrease the nitrate concentration of floodwaters and thereby reduce the nitrate load of adjacent rivers (Lindau et al. 1994; Tockner et al. 1999; Forshay and Stanley 2005). In contrast with non-tidal riparian floodplains where the duration of flooding ranges from 12 to 69 days year^{-1} (Tockner et al. 1999; Valett et al. 2005), TFZ floodplains are inundated twice-daily by tidal river flow. During these short duration (<6 h), high frequency (12–24 h) flooding events, TFZ floodplains also exchange all of their surface water with the river channel when water level recedes during low tide. These two characteristics of TFZs, high frequency inundation and complete hydrologic connectivity with the river, set these floodplains apart from others along the spectrum of river-floodplain interaction and may optimize conditions for nitrogen removal from TFZ rivers.

The goal of this study was to quantify denitrification flux from the TFZ riparian floodplain of a coastal river. This denitrification flux was compared with the riverine nitrate load to evaluate the potential importance of the floodplain in attenuating this load. We begin by presenting an empirical model that addresses the primary biogeochemical and geomorphic factors affecting floodplain denitrification.

Riparian zone denitrification model

Denitrification flux from TFZ riparian floodplain is a function of three elements: (1) the spatial and temporal extent of inundation, (2) denitrification rate, and (3) the lag time between inundation of the riparian sediments and the onset of denitrification. The first of these elements (the extent and duration of flooding) is a function of water level height and floodplain topography. Water level height, h, above mean sea level at any time, t, of the tidal cycle and location, s, along the TFZ is calculated as:

$$h_{t,s} = a_s \times \sin\left(\frac{2 \times \pi \times t}{p}\right) \quad (1)$$

where a_s is tidal amplitude specific to a location along the TFZ and p is the tidal period of 12.4 h. Floodplain topography determines the area inundated at any time (t) and location (s), $A_{t,s}$, such that:

$$A_{t,s} = h_{t,s} \times F_s \quad (2)$$

where F_s is a numerical function describing the area inundated at a given water level height for a particular location along the TFZ.

The second element that determines denitrification flux from the TFZ riparian floodplain is the area-specific denitrification rate (mass length^{-2} time^{-1}). The denitrification flux, N (mass time^{-1}) is the product of the denitrification rate, R, and the area

inundated (A). The final element controlling denitrification is the lag time, L, between the time that water inundates the riparian sediment and the initiation of denitrification. This lag time is due to the preferential use of O_2 over NO_3^- during microbial respiration; denitrification does not begin until O_2 is depleted in sediment porewater. After the lag time L expires, denitrification occurs on the portion of the floodplain that has been inundated for a period of time greater than L. The area of the floodplain in which anaerobic respiration occurs, and subsequent denitrification flux, continue to increase until the receding tide limits the denitrifying area. Calculation of the denitrification flux over a flood tide period (6.2 h) depends on two portions of the area inundation curve. The first period is between time zero of the flood tide and t_1 ($t_1 = (6.2 - L)/2$) when denitrification flux increases in proportion to the area inundated for greater than L. The second portion occurs between t_2 ($t_2 = t_1 + L$) and 6.2 h when the denitrification flux is limited by the receding tide. Denitrification flux within a segment of the TFZ floodplain is calculated as:

$$N_s = \int_{t_1}^{t_2} A_{t,s} \times R + \int_{t_3}^{6.2} A_{t,s} \times R \quad (3)$$

where $A_{t,s}$ is calculated at each time step using Eq. 2 with the $h_{t,s}$ and F_s specific for that location. The denitrification flux from the entire TFZ over the 6.2 h high tide is the summation of all N_s comprising the TFZ. Equation 3 incorporates all three of the principal controls on denitrification flux: topography, denitrification rate, and temporal lag in the onset of denitrification after tidal inundation.

This model is relevant to the surficial sediments where denitrification is interrupted by aerobic conditions during low tide. Denitrification in these surficial sediments during inundation directly affects the nitrogen concentration in the overlying floodplain water, and subsequently affects the nitrogen load of the river when this water drains back into the channel. While denitrification occurs in deeper sediment strata of the floodplain where reduced conditions occur continually, the influence of this process requires information on subsurface hydrology that was beyond the scope of this study.

Site description

The Newport River is a third-order blackwater stream in eastern North Carolina, U.S.A. that enters the Atlantic Ocean at Beaufort Inlet (Fig. 1). The 310 km^2 watershed drains unconsolidated late Cretaceous to Holocene sandy sediments (Phillips 1997); overall channel gradient from headwaters to estuary is 0.4 m km^{-1}. The 34 km^2 non-tidal upper watershed has predominantly agricultural and silvicultural land use. The TFZ drains an additional 128 km^2 of agricultural and light urban development. The TFZ is characterized by a semi-diurnal tide that propagates 8 km upstream from the oligohaline estuary (Fig. 1). The meandering, sand-bed channel is bordered by a wide riparian zone consisting of hardwoods (*Taxodium* spp, *Nyssa* spp, *Acer rubrum*, *Pinus* spp). Small pockets of tidal freshwater emergent marsh (*Peltandra virginica*, *Pontederia cordata*) are common along the entire length of the TFZ and grow on the muddy channel margin exposed at low tide. The riparian zone is inundated daily during the two high tides even during periods of low discharge (Fig. 2). Denitrification measurements were conducted approximately equidistant between the upper and lower bounds of the TFZ (Fig. 1). The average annual salinity was 0.07 in the vicinity of denitrification measurements and 0.25 at the downstream boundary of the tidal freshwater zone where the oligohaline river begins.

Materials and methods

Riparian zone denitrification

Denitrification rate of riparian zone sediments was measured to parameterize R in Eq. 3. Sediment cores were collected monthly from three intertidal habitats along the TFZ of the Newport River (Fig. 1). The three sample collection sites were located within 500 m of each other and included a hardwood riparian forest, an emergent freshwater marsh, and an unvegetated mudflat. Triplicate cores from each site were collected in clear polycarbonate tubes (6.4 × 40 cm). The sediment cores and 50 L of river water were returned to a temperature controlled room

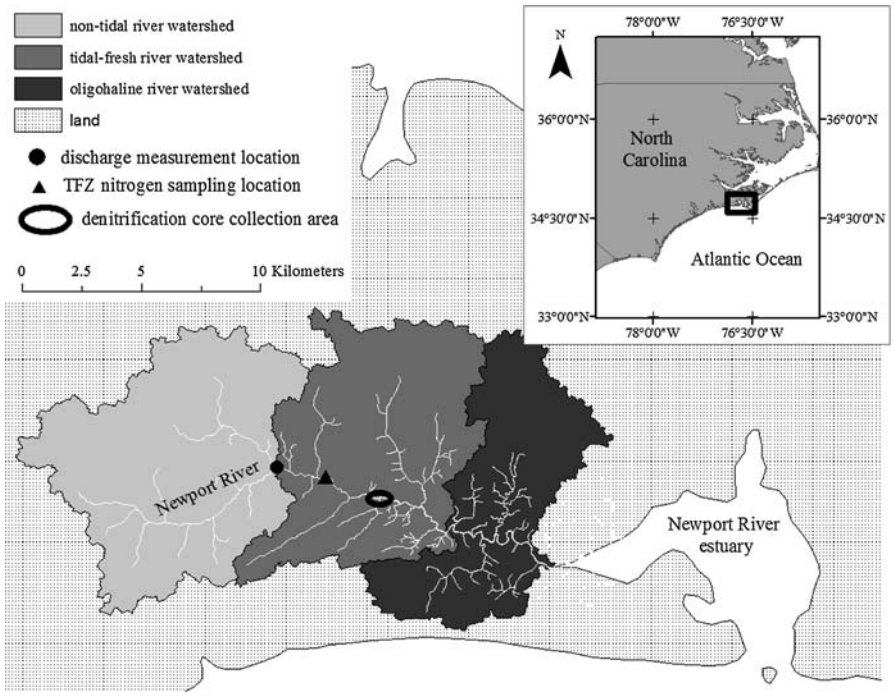

Fig. 1 Map of the Newport River watershed delineating the drainage areas of the non-tidal river, tidal freshwater river, and oligohaline estuary. Inset map shows the location of the Newport River in eastern North Carolina, USA

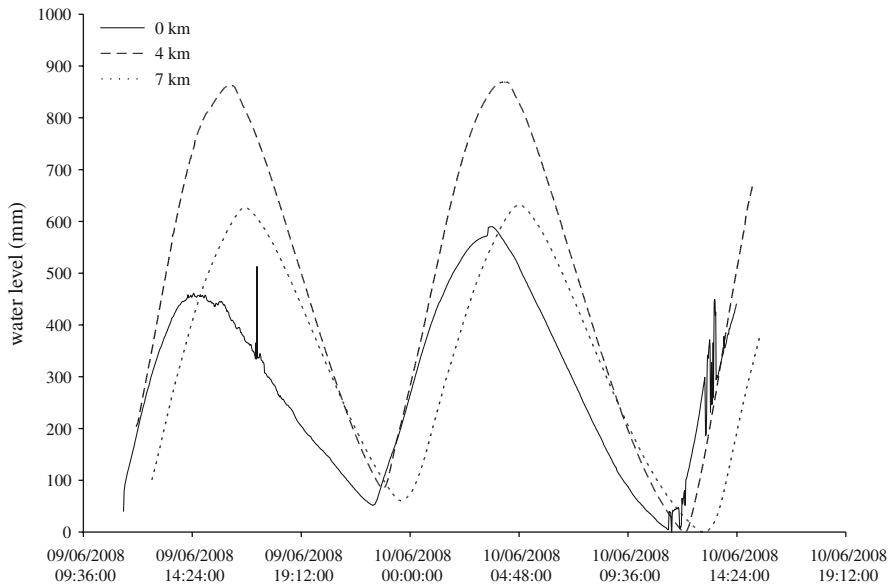

Fig. 2 Water level at three TFZ locations upstream from the oligohaline estuary of the Newport River, 9–10 June 2008. Values are relative to the lowest water level observed during the 1.2 day period at each location. Overbank flooding into the riparian zone was observed throughout the TFZ during this period despite the relatively low river discharge ($0.780\ m^3\ s^{-1}$). Water level was recorded at 5 min intervals using Intech WT-HR water height probe (Intech Instruments LTD, Christchurch, NZ)

at the University of North Carolina's Institute of Marine Sciences (UNC-IMS) maintained at the temperature of the river. Next, cores were filled with approximately 350 mL of river water and capped with air-tight lids containing two sampling ports. Cores were pre-incubated for >18 h prior to gas measurements to allow equilibration of dissolved gases within all materials (Eyre et al. 2002). For samples collected between August and November 2006 cores were incubated with a static volume of overlying water for 6 h and N_2 was measured in the overlying water every 2 h (Fear et al. 2005). A linear regression between N_2 concentration and incubation time was used to derive the rate of N_2 production

(denitrification) within the core. From December 2007 through August 2007 cores were plumbed to a multi-channel peristaltic pump that circulated river water through the headspace of the core at a known rate between 1 and 2 mL min^{-1} (McCarthy et al. 2007). Water samples for dissolved gas analysis were collected in 5 mL glass tubes from the inflow and outflow of the cores.

Dissolved gas analysis was measured using a Balzers Prisma QME 200 quadropole mass spectrometer (Pfeiffer Vacuum, Nashua, NH, USA) coupled to a silicon, gas-permeable, flow-through membrane inlet as described by Kana et al. (1994). The mass spectrometer was tuned to monitor the ratio of N_2:Ar instead of N_2 alone because the N_2:Ar signal is relatively unaffected by oxygen concentrations above 50% saturation (Kana and Weiss 2004; Fear et al. 2005). A continually-mixed water bath containing tap water at 16°C was maintained as an atmospheric gas-saturated standard for calibration of the mass spectrometer, where the [N_2]:[Ar] ratio of this water bath was 37.9266 (Lide 2004). This signal ratio ($(N_2{:}Ar)_{standard\ signal}$) was used to determine the N_2 concentration of the sample using the following formula:

$$[N_2]_{sample} = (N_2{:}Ar)_{sample\ signal} \times \frac{37.9266}{(N_2{:}Ar)_{standard\ signal}} \times [Ar]_{sample} \quad (4)$$

Since Ar is conservative and assumed to maintain a saturated concentration in water, standard gas saturation tables for a range of temperature in freshwater were used to obtain the $[Ar]_{sample}$ at the temperature of the incubation (Lide 2004).

Next, the denitrification rate (R, mass N $area^{-1}$ $time^{-1}$) occurring within the sediment core was calculated as:

$$R = 2 \times ([N_{2\,outflow}] - [N_{2\,inflow}]) \times \frac{q}{c} \quad (5)$$

where [$N_{2\ outflow}$] and [$N_{2\ inflow}$] are the [N_2] measured leaving and entering the core, respectively, q is the flow rate through the head space of the core, and c is the surface area of the core. Differences between sites during each experiment and overall during the period of study were examined using an ANOVA and Tukey post-hoc analysis ($p < 0.05$) with SPSS software (SPSS, Inc., Chicago, IL).

Calculation of denitrification from N_2 fluxes within sediment cores has a number of advantages over the more commonly used acetylene block method (Cornwell et al. 1999; Groffman et al. 2006). Most importantly, direct measurement of N_2 fluxes using a mass spectrometer does not interfere with coupled nitrification-denitrification as the acetylene block method does, thereby making denitrification rate measurements derived from N_2 fluxes more accurate. The resultant denitrification rates thus reflect both the benthic mineralization-nitrification-denitrification pathway and the denitrification of nitrate from the water column, but our methodology did not allow us to resolve the proportion of the total denitrification occurring by these pathways.

One drawback of the laboratory-based sediment core incubations performed in this study is that they reflect denitrification rates occurring when sediments are continually saturated and the sediment porewater O_2 has been depleted. In order to extrapolate the laboratory denitrification rates across the TFZ using Eq. 3, it was necessary to determine the lag time between inundation and the onset of denitrifying conditions. A combination of in-situ and laboratory measurements of oxidation-reduction potential (an indicator of O_2 availability and hence propensity of a sediment bacteria to denitrify NO_3^-) were performed to measure this lag time.

Riparian zone oxidation-reduction potential

In-situ measurements of oxidation-reduction potential in the TFZ riparian floodplain were conducted during winter (7 February–7 March 2007) and summer (27 July–13 August 2007) to measure the fluctuation between oxidized (>300 mV) and reduced (<300 mV) conditions. Oxidation-reduction potential of 300 mV was considered the threshold below which denitrification was likely to occur (Faulkner and Patrick 1992).

In-situ oxidation-reduction measurements were made during February and August 2007 at the TFZ riparian location where denitrification cores were collected. Platinum tipped probes (purchased from Dr. Wayne Hudnall at Texas Tech University) were deployed from a 17 m wooden boardwalk constructed perpendicular to the river. Two oxidation-reduction potential probes (5 and 10 cm below the

sediment/water interface) and one soil moisture probe (5 cm deep) were deployed at 2, 10, and 17 m from the low tide channel margin. Sensor depths and distances from the channel were chosen based upon observations reported in other TFZs (Kerner et al. 1990; Seybold et al. 2002). To minimize soil disturbance during deployment, a 15 cm deep hole was dug, oxidation-reduction potential and soil moisture probes were inserted laterally into the wall of the hole, and the hole was back-filled with the excavated soil.

Oxidation reduction robes were wired to a Campbell Scientific CR1000 data logger and measurements were recorded every 5 min. A Ag/AgCl reference electrode (Accumet 13-620-53) was connected to the sediment using a salt bridge (2 cm diameter PVC pipe filled with a gelled solution of agar and KCl) to provide an electrical ground for the oxidation-reduction potential measurements. Measured oxidation-reduction potential values were converted to Eh by adding 200 mV (per manufacturer's instructions); no temperature or pH corrections were made. Electrode calibration was verified by measuring a 220 mV oxidation-reduction potential solution: following the February deployment all probes read 220 ± 10 mV. Prior to and following the August deployments all probes read 261 ± 1 mV and 263 ± 2 mV, respectively. While the maximum stabilization period allowed by the data logger was used for voltage measurements (3,000 ms), it may not have been long enough to allow the voltage to stabilize in strongly reduced sediments (0–200 mV) (van Bochove et al. 2002). Values in this range may be an underestimate of oxidation reduction potential by up to 140 mV (van Bochove et al. 2002).

Soil moisture was measured as an indicator of the tidal inundation of the sediment that could be compared against the oxidation-reduction potential data. Furthermore, soil moisture indicates the propensity for denitrification to occur and the extent of nitrate reduction (N_2O versus N_2) (Machefert and Dise 2004). Soil moisture probes (model CS616, Campbell Scientific, Incorporated, Logan, UT, USA) were calibrated according to the manufacturer's instructions and installed at 5 cm depth at each of the three distances from the river channel. Probes were wired to the data logger and volumetric soil moisture was recorded every 5 min.

Laboratory oxidation-reduction potential experiments

As a compliment to the in-situ measurements described above, a laboratory experiment was conducted in January 2008 to assess the time required for oxidized (drained) sediments to become reduced after inundation (lag time parameter, L, in Eq. 3). The experimental design was based on the observation from in-situ monitoring that large oxidation-reduction potential fluctuation only occurred within the upper 5 cm of the sediment profile. Accordingly, soil cores 6 cm in depth were collected from the boardwalk described above and returned to the UNC-IMS. Oxidation-reduction potential probes were inserted into the cores through holes at 1, 2, 3, and 5 cm, while a second hole at each depth allowed lateral water infiltration. Oxidation-reduction potential was measured and logged as described for the in-situ measurements. In a series of experiments, the instrumented sediment cores were incubated at 10 and 25°C in a temperature controlled room and were initially allowed to drain until a constant oxidation-reduction potential condition was observed. Cores were then submerged in river water equilibrated to the temperature of the experiment and the time required for oxidation-reduction potential to drop below 300 mV (reducing conditions amenable for denitrification; Faulkner and Patrick 1992) was measured.

Channel bathymetry and riparian zone topography

Channel width and cross-section area were measured from a boat along the TFZ during high tide at 28 locations. These surveys only spanned the channel between vegetated banks, so digital elevation data was used to develop a topographic surface of the riparian zone beyond the banks of the channel. Topographic Light Image Detection and Ranging (LIDAR) data were obtained for the Newport River watershed from the North Carolina Floodplain Mapping Agency (www.ncfloodmaps.com). These elevation data have a vertical root mean square error of 20 cm and the NAVD 88 vertical datum on which the data are based is 9 cm below mean sea level for the Newport River (as determined using Vdatum software, http://vdatum.noaa.gov/). ArcGIS (ESRI, Redlands, CA, USA) software was used to construct a

triangulated irregular network (TIN) from the LIDAR data within 50 m of the river channel (tributaries were not included in this analysis). A zero elevation hard break line was forced along the river channel to represent the river surface at mean sea level and a soft break line was enforced at 50 m from the channel. The surface area of this TIN at 0.03 m intervals between mean sea level and 0.45 m in elevation was calculated for 9, 1 km reaches of the TFZ using ArcGIS.

The change in inundated surface area with elevation above mean sea level (F_s, Eq. 2) was represented by fitting a polynomial regression to the modeled points for each river reach; r^2 values for all regressions were >0.999. This topographic model was used to generate a relationship between water level height ($h_{t,s}$, Eq. 1) and the area ($A_{t,s}$, Eq. 2) of floodplain inundated within 50 m of the river channel. Inundation may occur beyond 50 m, but we choose this conservative boundary for two reasons. First, lateral flow velocity of water from the channel into the riparian zone will limit the extent of inundation, but was not measured in this study. Second, we wanted to minimize consideration of ponds in the outer floodplain that would not be expected to exchange water with the river channel.

Tidal freshwater river nitrogen load

Nitrate, ammonium, and total nitrogen concentration were measured twice-monthly from river water collected during the ebb tide in the upper TFZ (Fig. 1). Aqueous nitrogen analyses were performed on a Lachat QuikChem 8000 autoanalyzer (Lachat Instruments, Milwaukee, WI, USA) at the UNC-IMS. River discharge was measured monthly 100 m upstream of the TFZ using a Sontek handheld acoustic doppler velocimeter (SonTek/YSI, San Diego, CA, USA) to measure velocity at 1 m intervals across the channel. An area-specific discharge was calculated for the watershed at this non-tidal location and used to estimate discharge downstream at the location where river nitrogen was measured (Leopold et al. 1964). River nitrogen load in the upper TFZ was calculated as the product of discharge and river water nitrogen concentration measured on the date closest to when discharge was measured.

Riparian zone denitrification model

The total denitrification flux of nitrogen from the riparian TFZ (kg N day^{-1}) was calculated using Eq. 3 on a monthly basis, resulting in 11 estimates of denitrification flux over the year of study. For each month, the average denitrification rate of the three intertidal habitats was used to extrapolate across the entire TFZ riparian area. Equation 3 was implemented at a 0.1 h time step for each of the 9 reaches of the TFZ using water level height-inundated area relationships (F_s) specific to that reach. Denitrification flux (N_s, Eq. 3) over the 6.2 h period was numerically integrated for each reach, and N_s for all 9 reaches was summed to obtain N for the entire TFZ. These flux estimates only account for denitrification occurring above mean sea level and therefore do not include denitrification occurring in the portion of the channel inundated continuously throughout the tidal cycle.

Results

Riparian zone denitrification

Denitrification rates ranged from 233 μg m^{-2} h^{-1} (mud flat in September 2006) to 4,418 μg m^{-2} h^{-1} (riparian forest in October 2006) (Table 1). There was a significant difference ($p < 0.05$) between habitat types during September and October 2006, with rates from the forest higher than rates at the mudflat; no other significant differences were found between habitats during the same month. Denitrification over the 11 months of study averaged 2018, 1832, and 1956 μg m^{-2} h^{-1} at the forest, marsh, and mud flat, respectively, and these differences were not statistically significant ($F_{2,30} = 0.057$, $p = 0.944$) (Table 1). No significant difference was found between the monthly averages of the three habitats over the year of study ($F_{10,22} = 2.21$, $p = 0.058$).

Ambient water temperatures and subsequent incubation temperatures of denitrification experiments ranged from 9.7 to 25.5°C (Table 2). The ranges in dissolved nitrogen concentrations were 93–450 μg $N–NO_3^-$ L^{-1}, 12–58 μg $N–NH_4^+$ L^{-1}, and 140–982 μg N–dissolved organic L^{-1} (Table 2). Average organic matter in the top 5 cm of sediment of incubated cores was highest in the forest (19%),

Table 1 Nitrogen generation (μg N m^{-2} h^{-1} from intertidal sediments in three riparian habitats of the Newport River, NC; values are mean ± 1 SD

Date	Forest	Vegetated wetland	Mud flat	Habitat average
31 Aug 2006	–	1,669 ± 1,592	2,731 ± 552	2,200 ± 751
14 Sep 2006	1,535 ± 588^{A}	1,428 ± 210^{AB}	233 ± 359^{C}	1,065 ± 722
24 Oct 2006	4,418 ± 45^{A}	3,250 ± 1,267^{AB}	1,626 ± 525^{C}	3,098 ± 1,402
21 Nov 2006	4,177 ± 1,952	2,517 ± 420	1,796 ± 608	2,830 ± 1,221
14 Dec 2,006	675 ± 645	957 ± 743	2,108 ± 526	1,247 ± 759
18 Jan 2007	1,226 ± 159	2,261 ± 1,040	2,925 ± 629	2,137 ± 857
14 Feb 2007	883 ± 1,464	2,006 ± 1,503	3,753 ± 533	2,214 ± 1,446
7 Mar 2007	1,750 ± 292	1,508 ± 323	1,315 ± 134	1,524 ± 218
16 May 2007	1,998 ± 1,232	732 ± 473	1,310 ± 199	1,347 ± 634
31 Jun 2007	2,784 ± 977	2,806 ± 1,156	2,683 ± 1,415	2,758 ± 65
8 Aug 2007	735 ± 566	1,379 ± 285	1,039 ± 208	1,051 ± 322
Annual average	2,018 ± 1,361	1,865 ± 781	1,956 ± 1,005	–

Letters indicate homogenous subsets of treatments during each month found to differ by ANOVA and Tukey post-hoc analysis ($p < 0.05$)

followed by the marsh (11%), and mudflat (10%) (Table 2).

Riparian zone oxidation-reduction potential

The channel bank (2 m from the low tide channel) during winter had dramatic oxidation-reduction potential fluctuations at 5 cm soil depth between oxidized (>300 mV) and reduced (<300 mV) conditions that were inversely related to changes in soil moisture (Fig. 3a). During 25 Feb through 2 Mar, reduction of sediments from an oxidized condition to <300 mV required 4 h 40 min. Sediments at 10 cm depth were continually reduced and showed little fluctuation during winter. Oxidation-reduction potential decreased with distance from the channel during winter and oxidation-reduction potential values at 5 and 10 cm were similar to one another (Figs. 4a, 5a). At 10 m from the channel, oxidation-reduction potential at both 5 and 10 cm showed small semi-diurnal fluctuations that were inversely related to soil moisture fluctuations (Fig. 4a). This pattern was dampened even further at 17 m from the channel except during the final 4 days of this period when a rain event on 1–3 March coincided with rapid semi-diurnal changes in oxidation-reduction potential at 5 cm (Fig. 5a).

Oxidation-reduction potential was generally lower in summer than winter. Nearest the channel, oxidation-reduction potential at 5 cm fell rapidly following rain events on 30–31 July and 2 August (Fig. 3b). These upper sediments remained highly reduced (<0 mV) except during 3 instances of low soil moisture when oxidation-reduction potential temporarily spiked to ~150 mV. Sediments at 10 cm during summer fell from ~200 to ~−50 mV following rain events on 2 and 6 August (Fig. 3b). Oxidation-reduction potential 10 m from the low tide channel decreased over time, with significant changes coinciding with rain events on 30–31 July and 2 August (Fig. 4b). The 2 August rain event corresponded with a large decrease in oxidation-reduction potential at the site farthest from the channel (Fig. 5b). By the end of August both riparian sites showed similar oxidation-reduction potential conditions without large vertical gradients (Figs. 4b, 5b). Given the highly reduced conditions during August, the oxidation-reduction potential measurements may under-represent true conditions (van Bochove et al. 2002). However, since values were mostly below 150 mV, under-estimation by 140 mV would not interfere with the detection of oxidized (>300 mV) to reduced (<300 mV) fluctuations.

Volumetric soil moisture was generally higher during winter than summer and showed a semi-diurnal pattern at all sites and seasons that reflected the tidal influence (Figs. 3, 4, 5). Soil moisture changed by <1% v/v over a tidal cycle at all sites and

Table 2 Water column nitrogen concentrations and sediment organic matter composition during denitrification experiments

Date	Habitat	Temperature (°C)	NO_3 (μg N L^{-1})	NH_4 (μg N L^{-1})	Organic N (μg N L^{-1})	% Organic matter
31 Aug 2006	Marsh					10.8
	Mudflat	25.0	369	45	140	10.8
	Forest					No data
14 Sep 2006	Marsh					8.7
	Mudflat	22.0	93	37	No data	7.7
	Forest					14.3
24 Oct 2006	Marsh					8.1
	Mudflat	15.5	220	21	No data	6.7
	Forest					15.9
21 Nov 2006	Marsh					No data
	Mudflat	14.0	178	30	982	No data
	Forest					No data
14 Dec 2006	Marsh					14.9
	Mudflat	9.7	175	28	348	9.8
	Forest					19.8
18 Jan 2007	Marsh					17.9
	Mudflat	12.2	124	24	323	21.1
	Forest					25.9
14 Feb 2007	Marsh					10.6
	Mudflat	10.0	144	58	318	10.4
	Forest					32.4
7 Mar 2007	Marsh					12.9
	Mudflat	11.9	450	23	326	4.1
	Forest					8.0
16 May 2007	Marsh					7.0
	Mudflat	19.8	161	12	424	8.6
	Forest					15.4
31 Jun 2007	Marsh					8.2
	Mudflat	25.5	294	19	415	11.9
	Forest					24.1
8 Aug 2007	Marsh					7.1
	Mudflat	28.0	29	21	558	9.2
	Forest					28.5

seasons, indicating that the soils were poorly drained during low tide. Rain events were not reflected in the soil moisture data presumably because the soils maintained a near-saturated condition continuously due to tidal inundation. Throughout the study period volumetric soil moisture was >50%, corresponding with the highest denitrification rates in a wide variety of ecosystems and the maximum N_2 versus N_20 production (Machefert and Dise 2004).

Laboratory oxidation-reduction potential experiments

Manipulation of water level in sediment cores in the laboratory revealed time lags between oxidized and reduced conditions consistent with those observed in-situ. The laboratory experiment conducted at 10°C did not show a dramatic response in oxidation-reduction at 1–2 cm in depth. However, at 3 cm, the

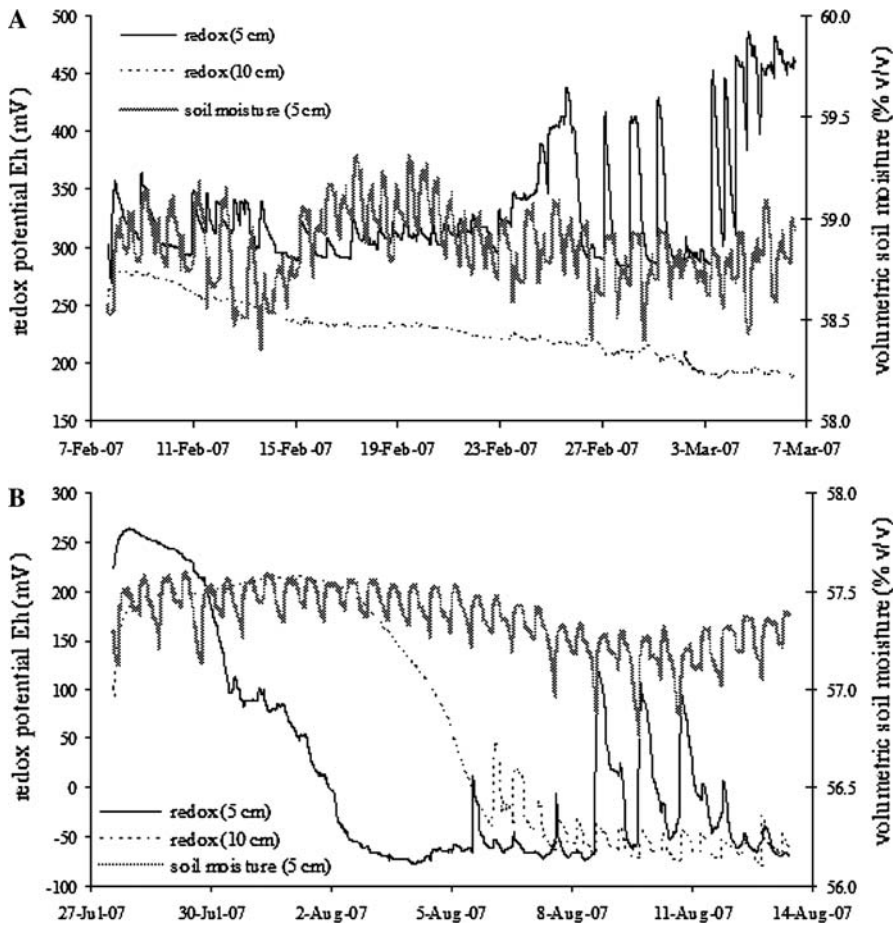

Fig. 3 Oxidation-reduction potential and soil moisture 2 m from the channel of the Newport River during **a**. February–March 2007 and **b**. July–August 2007

sediment took 4 h and 40 min to become reduced from an oxidized condition (Fig. 6a). This lag period between inundation and denitrifying conditions is the same as that observed in-situ during 25 Feb–2 Mar (Fig. 3a). At 25°C, 5 h 10 min was required for the sediments at 1 cm to become reduced from a fully oxidized condition; sediments below that depth were never fully oxidized (Fig. 6b). Given the agreement between field and laboratory measurements in lag time of 4 h 40 min, this value was used to parameterize L in Eq. 3.

Channel bathymetry and riparian zone topography

The aerial extent of the TFZ river channel at low tide was 149,360 m^2, while the maximum inundated area at high tide was 426,627 m^2. The surface area of riparian floodplain inundated during the flood tide was greatest in the middle and upper portion of the TFZ, between 3 and 7 km from the oligohaline estuary (Figs. 7, 8a).

Tidal freshwater river nitrogen load

In the upper TFZ, low river discharges <1 $m^3\ s^{-1}$ occurred during April–June of 2006 and 2007; peak discharges of 4.8 $m^3\ s^{-1}$ occurred in September 2006 following Hurricane Ernesto and 4.9 $m^3\ s^{-1}$ in December 2006 (Fig. 9). Nitrate, ammonium, and organic nitrogen in the upper portion of the TFZ averaged 53 $\mu g\ L^{-1}$, 46 $\mu g\ L^{-1}$, and 399 $\mu g\ L^{-1}$, respectively during the study period (Fig. 9). Average nitrate concentration in the middle TFZ where denitrification rates were measured (see Fig. 1) was 203 $\mu g\ L^{-1}$ (Table 1), fourfold higher than the average in the upper TFZ (53 $\mu g\ L^{-1}$). A sewage treatment plant outfall near the study site may be partly responsible for the increased nitrate

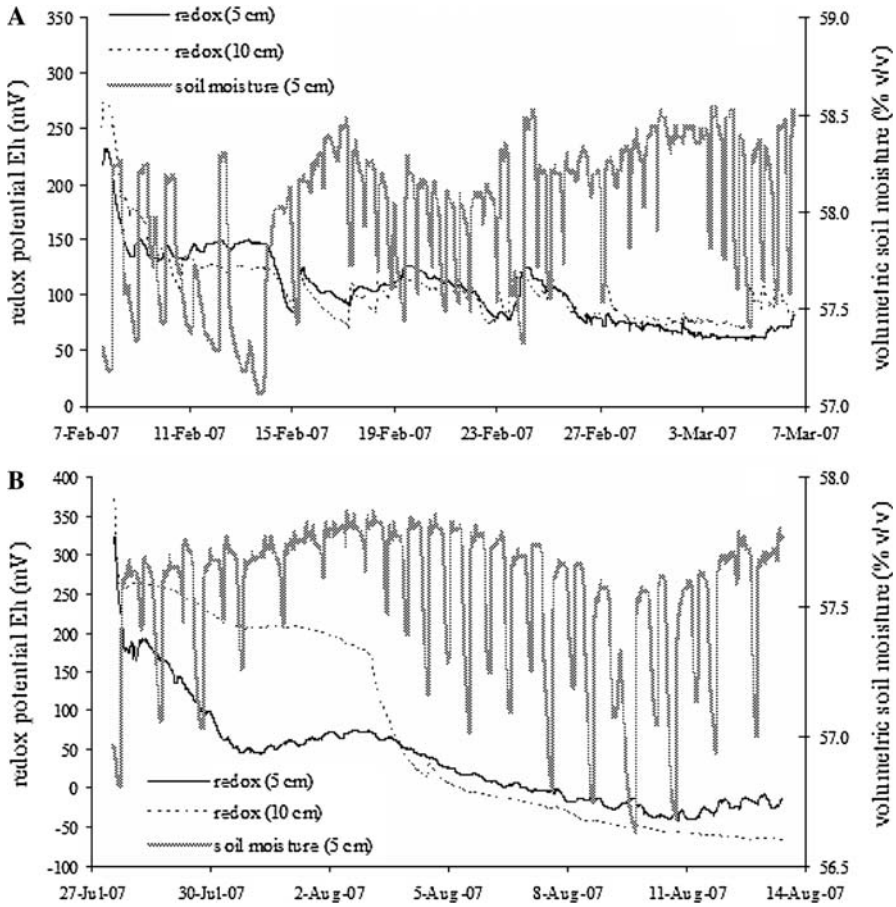

Fig. 4 Oxidation-reduction potential and soil moisture 10 m from the channel of the Newport River during **a**. February–March 2007 and **b**. July–August 2007

concentration; total nitrogen load from the treatment plant was similar to the riverine total nitrogen load during low flow periods (Ensign, unpublished data).

Riparian zone denitrification model

Denitrification flux was greatest in the middle and upper portion of the TFZ where inundated area was greatest (Fig. 8b is representative of the trend in denitrification over time and space, although the magnitude of this flux changed from month to month). The peaked pattern shown in Fig. 8b is a consequence of the lag time (4.6 h) implemented in Eq. 3, the increase in wetted surface after this lag time, and the subsequent decrease in wetted surface area and denitrification as the water level receded. Denitrification flux from the TFZ riparian area ranged from 0.200 kg N per lunar day (24.8 h) in August 2007 to 0.589 kg N per lunar day in October 2006 (Table 3). As a proportion of the daily riverine nitrate load entering the upper portion of the TFZ, these denitrification fluxes ranged from 2% in September 2006 to 262% in May 2007 (Table 3). The high removal capacity predicted in May 2007 was a result of extremely low river discharge and thus low riverine nitrogen load (Fig. 9).

Discussion

Semi-diurnal changes in water level in a tidal freshwater river in coastal North Carolina resulted in a threefold expansion in riverine surface area from low tide to high tide. Denitrification within three intertidal habitats of the river's riparian zone occurred at similar rates, which varied threefold over an annual period. The onset of denitrification in surficial sediments occurred 4–5 h after inundation by the flood tide. Denitrification flux from the floodplain was estimated to constitute between 2

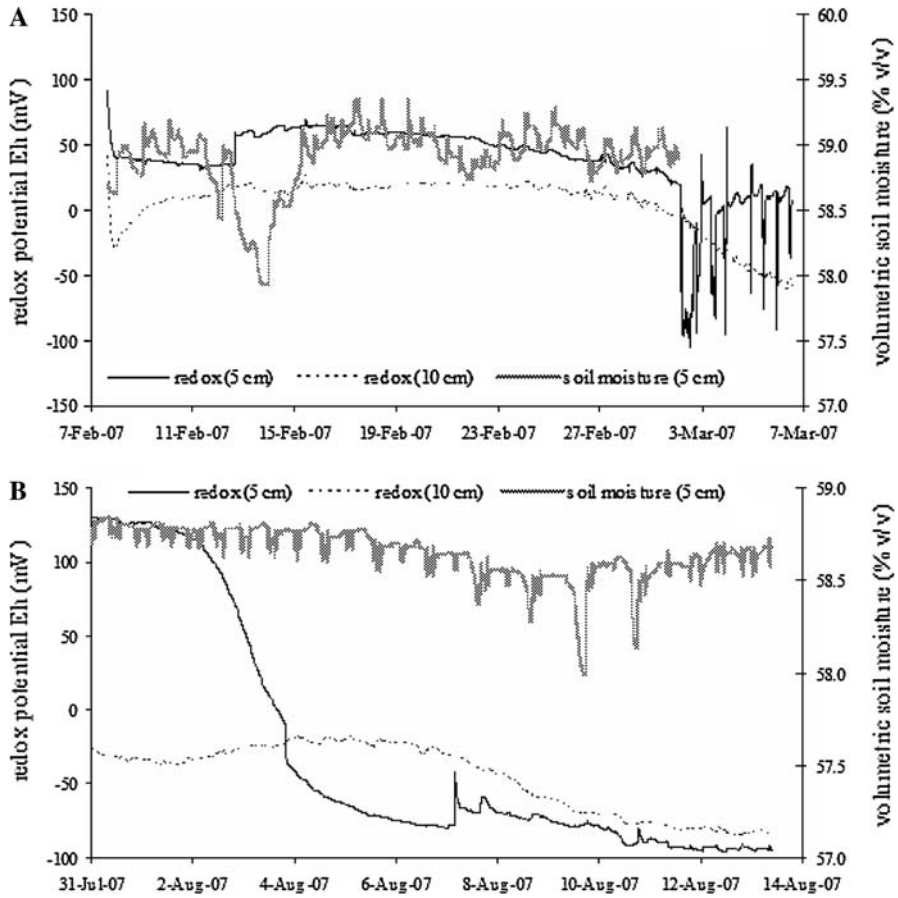

Fig. 5 Oxidation-reduction potential and soil moisture 17 m from the channel of the Newport River during **a**. February–March 2007 and **b**. July–August 2007

and 15% of the daily in-channel riverine nitrate load during most of the year, and >100% during periods of low river discharge. Since these floodplains are inundated twice daily by river water from the channel, they are unique relative to non-tidal floodplains that flood only seasonally. This regularly occurring, direct hydrologic exchange between river channel and floodplain results in a continuous, year-round loss of nitrogen from the tidal freshwater portion of this coastal river.

Denitrification and redox dynamics in tidal freshwater river floodplains

The current study is the first to quantify the effect of denitrification occurring across an entire tidal freshwater riparian zone on the nitrogen budget of a tidal freshwater river. Most previous research on TFZ environments has been done on nitrogen cycling within emergent freshwater marshes. For example, the annual net flux of nitrate to the riparian zone of a Massachusetts coastal river was 5% of riverine load, although the portion of this flux that was denitrified was not well constrained in the budget (Bowden et al. 1991). A TFZ marsh in Virginia was also an annual net sink for riverine nitrate where denitrification (42%) and burial (52%) accounted for permanent nitrogen loss; however, the net affect of this on riverine load was not calculated (Neubauer et al. 2005). Other TFZ studies have carefully analyzed nitrogen uptake and transformations within a TFZ marsh, but were not able to assess the impact of denitrification on the ecosystem NO_3^- budget. Our intention was not to disregard the complexity of nitrogen transformations documented in these earlier studies, but to focus on the net effect of the TFZ on nitrogen cycling within the river continuum.

The denitrification rates measured in the Newport River TFZ are similar to those reported in a Virginia TFZ marsh (Neubauer et al. 2005), slightly higher than those reported in some European TFZ floodplain

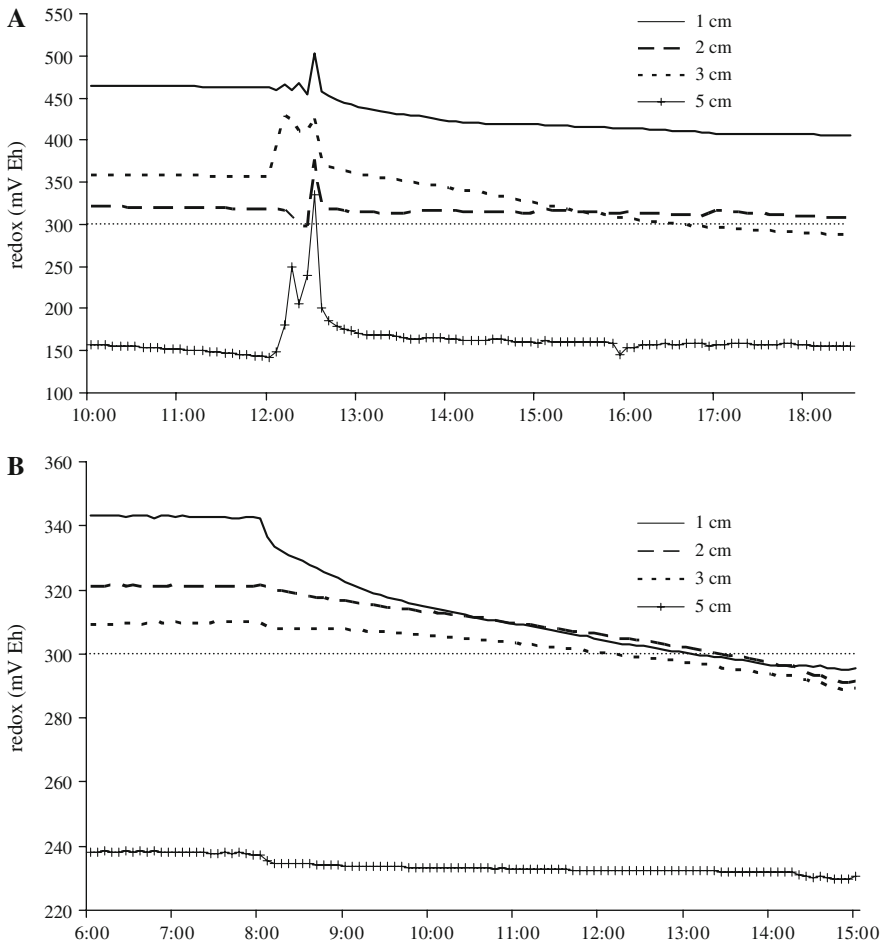

Fig. 6 **a**. Laboratory soil core oxidation-reduction potential experiment at 10°C; core was submerged at 12:00, and **b**. laboratory soil core oxidation-reduction potential experiment at 25°C; core was submerged at 08:00. The gray line marks the transition between oxic and reduced conditions

environments (Verhoeven et al. 2001), but lower than those reported in a Belgium TFZ marsh (Gribsholt et al. 2006). Floodplains can have high spatial and temporal heterogeneity in denitrification rates (Orr et al. 2007) as a result of variable soil characteristics and geomorphology (Pinay et al. 1995; Pinay et al. 2000), soil moisture (Machefert and Dise 2004; Pinay et al. 2007), temperature, and nitrate concentration (Pinay et al. 2007). Rates in this study were usually similar between habitats due to the relatively similar sediment organic matter content, water column nitrate concentration, and incubation temperature during experiments. Relative to non-tidal floodplains, tidal freshwater floodplains may have relatively homogenous denitrification rates as a result of similar soils, soil moisture regimes, and flooding.

Oxidation-reduction potential was used as an indicator of when denitrification would likely occur in the tidal freshwater riparian zone. In situ measurements showed that the upper 5 cm of sediment was predominantly oxic during winter along the channel edge, likely due to cooler temperatures than summer. Sites farther from the channel never showed oxidized conditions during winter or summer, perhaps due to low topographic relief and subsequently slow local groundwater movement. Laboratory experiments examined finer-scale responses within the upper 5 cm of sediment, showing that between 4.3 and 5.2 h were required for the oxic-to-reduced transition. Both in situ and laboratory experiments demonstrated that sediments were generally more reduced at higher temperatures, and that oxidation-reduction potential at a given depth in the sediment was more dynamic at higher temperature.

With respect to the oxidation-reduction dynamics considered in our model, we assumed that exposed surficial sediments in this active zone equilibrated to 350 mV as indicated by our in-situ monitoring

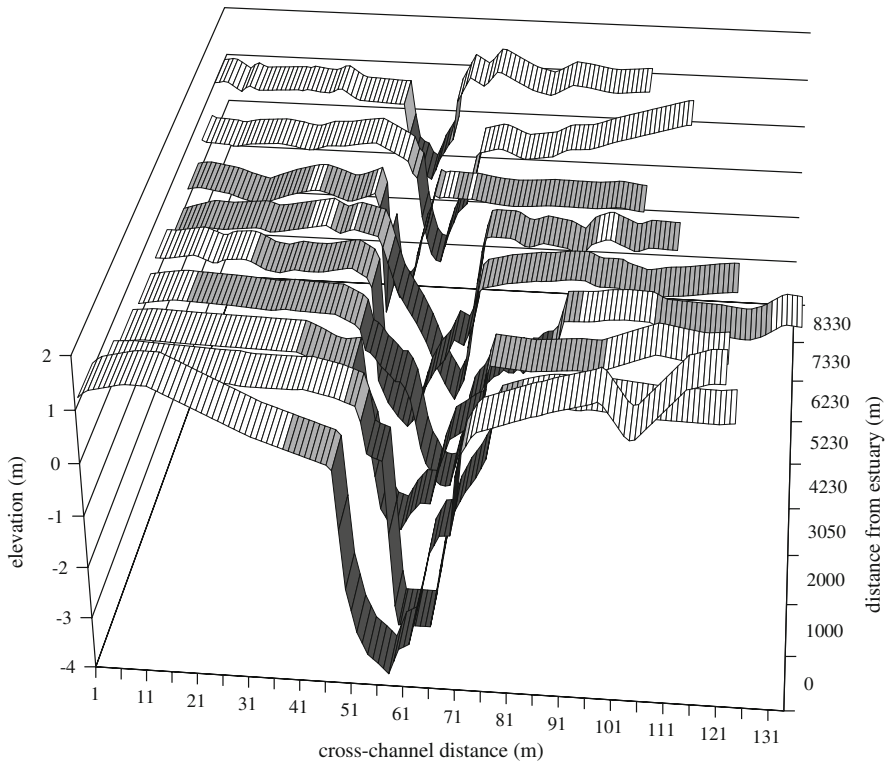

Fig. 7 Bathymetry and topography of the Newport River tidal freshwater zone from merged LIDAR and cross-section survey data. Dark gray represents low-tide wetted channel, light gray represents high tide wetted riparian zone, and white represents upland non-inundated area

(Fig. 3a), laboratory based oxidation-reduction potential experiments (Fig. 6), and other studies (Kerner et al. 1990). Other sediment types may achieve a higher oxidation-reduction potential during exposure to air, thereby increasing the lag time (*L*, Eq. 3) prior to the onset of denitrification. For example, the lag period of 7 days was reported for a Mississippi wetland (Lindau et al. 1994). Longer lag time would decrease the denitrification flux from the TFZ floodplain, while shorter lag time would increase denitrification flux.

Uncertainties, future development, and application of the floodplain denitrification model

There are several uncertainties in our parameterization of the denitrification model which may have resulted in either under- or over-estimating denitrification. Our model estimates may be under-estimates of denitrification flux for three reasons. First, nitrification occurs during the oxidized phase of the tidal cycle as found in other TFZ studies (Gribsholt et al. 2006), and this nitrate is subsequently denitrified when sediments are inundated. While our denitrification measurements included coupled nitrification-denitrification occurring in the cores, our experimental approach did not replicate the pulse of nitrate that occurs under field conditions during low tide. This additional nitrate would increase the denitrification rate and consequently the N_2 flux from the riparian zone. Second, the inundated riparian zone may be wider than the 50 m width we accounted for with the digital topographic model. Third, the lag time that was implemented in the model was based upon oxidation-reduction measurements in the upper 5 cm of sediment, although oxidation-reduction data suggest denitrification occurred in deeper sediments, as well. Since the intention of the model was to estimate nitrate removal from the overlying water column, we focused on the upper 5 cm of the sediment profile whose oxidation-reduction potential responded quickest following inundation. Consideration of denitrification occurring in the continuously reduced sediments below 5 cm would increase the expected nitrate removal in the TFZ floodplain, but we do not currently have data on riparian groundwater dynamics to evaluate this process. Lastly, the model may have over-estimated denitrification in the

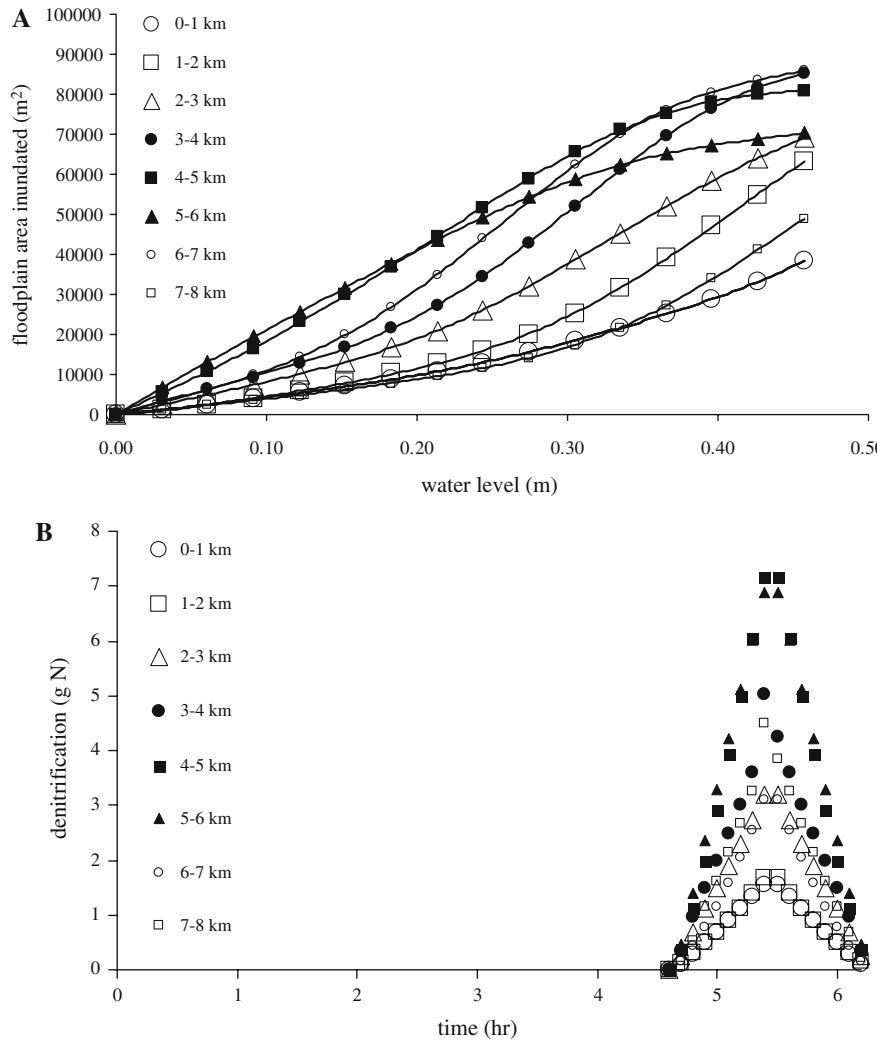

Fig. 8 **a**. Results of the GIS topographic analysis of river floodplain morphology along nine 1-km river segments of the Newport River extending from the oligohaline estuary to the top of the TFZ, and **b**. denitrification within the Newport River TFZ during June 2007 estimated using Eq. 3

TFZ since the denitrification rates used for extrapolation were based on water column nitrate concentrations that were higher than elsewhere along the river; lower water column nitrate concentrations would result in lower denitrification rates (Garcia-Ruiz et al. 1998).

Future development of the our model would involve research to address the uncertainties identified above and implementation of more spatially-explicit information from the riparian zone. First, spatial delineation of the floodplain into habitat types would allow explicit consideration of denitrification rates and oxidation-reduction dynamics within habitats in the proportion and configuration that they occur across the floodplain. Second, data on the relationship between river discharge and the extent of overbank flooding in the TFZ would improve estimates of inundated area during seasonal cycles of discharge regime.

The denitrification flux modeling framework presented here can be widely applied to generate estimates of nitrogen loss from coastal rivers worldwide. This exercise would serve two purposes. First, it would provide data on nitrogen attenuation rates along a missing link in the river continuum which is not currently accounted for in river network nitrogen models (see comparison of riparian versus in-channel denitrification below). Second, it would enable analysis of the effects of floodplain topography and river geomorphology on nitrogen dynamics in rivers. The current model could be useful in addressing many critical questions regarding of nitrogen flux through

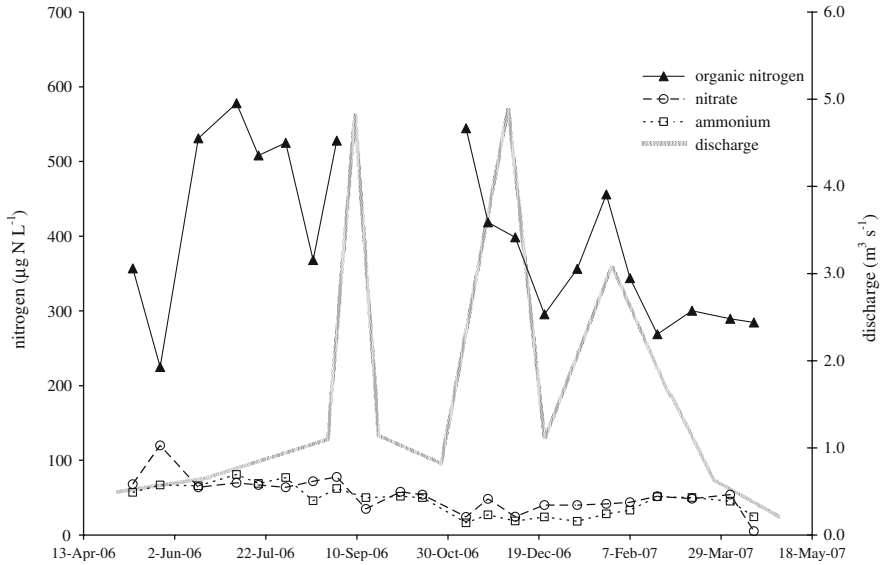

Fig. 9 Nitrogen concentrations and net downstream discharge in the upper TFZ Newport River, NC, April 2006–April 2007

tidal freshwater rivers, such as: Does inundated surface area (and subsequent denitrification flux) scale proportionally to river size? What is the relative importance of denitrification rate versus floodplain area in affecting riverine nitrogen loads? The denitrification model presented here provides a tool to efficiently pursue these questions and advance our understanding of nitrogen flux through tidal freshwater rivers.

How does riparian denitrification compare to in-channel denitrification?

Nitrogen uptake within river networks does not normally include riparian zone processes since overbank flooding in non-tidal rivers is a periodic event on annual time-scales. The current study indicates that exclusion of riparian zone denitrification in a riverine nitrogen uptake model of the Newport River would

Table 3 Nitrate loads, denitrification flux, and nitrate removal in the TFZ Newport River, NC

Riverine nitrate load		Riparian denitrification flux		Proportion of riverine nitrate denitrified in riparian zone (%)	Proportion of riverine nitrate denitrified in-channel[a] (%)
Date	kg lunar day^{-1}	Date	kg lunar day^{-1}		
25 Aug 2006	7.706	31 Aug 2006	0.418	5	13
9 Sep 2006	15.024	14 Sep 2006	0.203	2	8
22 Sep 2006	3.613				
26 Oct 2006	3.969	24 Oct 2006	0.589	15	21
2 Dec 2006	10.734	21 Nov 2006	0.538	5	4
22 Dec 2006	4.053	14 Dec 2006	0.237	6	19
28 Jan 2007	11.436	18 Jan 2007	0.406	4	7
1 Mar 2007	7.435	14 Feb 2007	0.421	6	9
		7 Mar 2007	0.290	4	12
29 Apr 2007	0.098	16 May 2007	0.256	262	94
No data	No data	30 Jun 2007	0.524	No data	No data
No data	No data	8 Aug 2007	0.200	No data	No data

Nitrate loads were calculated from discharge and concentration in the upper TFZ. A lunar day lasts 24.8 h

[a] The proportion of riverine nitrate load denitrified in-channel (R) was estimated as: $R = 1 - \exp(V_f/H_L)$, where H_L = discharge/(channel width × reach length) (Wollheim et al. 2006). Channel width was assumed to be 16 m and reach length was 8,000 m. The denitrification mass transfer coefficient, V_f, was estimated from river NO_3^- concentration using the formula $V_f = -0.493 \times \log[NO_3^-] - 2.975$ (Mulholland et al. 2008). V_f values ranged from 1.2×10^{-4} to 4.8×10^{-4} cm s^{-1}

underestimate nitrate uptake, but to what extent? As a first approximation, an empirical model of river nitrogen attenuation (Wollheim et al. 2006; Wollheim et al. 2008) can be applied to the TFZ of the Newport River. This model predicts that benthic in-channel denitrification occurring throughout the tidal cycle removed 4–94% of the daily riverine nitrate load over the course of this study (Table 3). Our estimates of riparian zone denitrification ranged from 27 to 278% of this in-channel denitrification, reflecting the importance of the riparian zone to overall nitrogen attenuation. On average, calculation of riverine nitrate attenuation without consideration for riparian denitrification would under-estimate nitrate attenuation in the TFZ by 38%.

Future efforts to model river network nitrogen attenuation can be improved by consideration of the additional nitrogen attenuation that occurs in the TFZ of coastal rivers, and the model presented here may provide a starting point for this research. Ultimately, the goal of this research should be the development of generalized empirical relationships between tidal freshwater river geomorphology and nitrogen attenuation similar to those developed for non-tidal rivers (see footnote of Table 3 for discussion of existing methodology). These data will fill a missing biogeochemical link along the riverine continuum and lead to improved accuracy of nitrogen budgets at the regional and global scale.

Acknowledgments Funding was provided by the Water Resources Research Institute of the University of North Carolina (Project # 70223), NSF Career Award #0441504 (M.W.D.), EPA STAR Graduate Fellowship #FP-91686901-0 (S·H.E.), and NSF EAR-0815627 (M.F·P.). We thank Ashley Smyth, Suzanne Thompson, Laura Stephenson, Nicholas Politte, Karen Fisher, Valerie Brock, and Todd Jobe for field and laboratory assistance, and Dr. Hans Paerl and his staff for the use of analytical equipment at UNC-IMS. Claude Lewis and Joe Purifoy at the UNC-IMS provided logistical support. The research described in this paper has been funded wholly or in part by the United States Environmental Protection Agency (EPA) under the Science to Achieve Results (STAR) Graduate Fellowship Program. EPA has not officially endorsed this publication and the views expressed herein may not reflect the views of the EPA.

References

Bowden WB, Vörösmarty CJ, Morris JT, Peterson BJ, Hobbie JE, Steudler PA, Moore B (1991) Transport and processing of nitrogen in a tidal freshwater wetland. Water Resour Res 27:389–408. doi:10.1029/90WR02614

Boyer EW, Alexander RB, Parton WJ, Li C, Butterbach-Bahl K, Donner SD, Skaggs RW, Del Grosso SJ (2006) Modeling denitrification in terrestrial and aquatic ecosystems at regional scales. Ecol Appl 16(6):2123–2142. doi:10.1890/1051-0761(2006)016[2123:MDITAA]2.0.CO;2

Cornwell JC, Kemp WM, Kana TM (1999) Denitrification in coastal ecosystems: methods, environmental controls, and ecosystem level controls, a review. Aquat Ecol 33:41–54. doi:10.1023/A:1009921414151

Destouni G, Hannerz F, Prieto C, Jarsjö J, Shibuo Y (2008) Small unmonitored near-coastal catchment areas yielding large mass loading to the sea. Global Biogeochem Cycles. doi:10.1029/2008GB003287

Eyre BD, Rysgaard S, Dalsgaard T, Christensen PB (2002) Comparison of isotope pairing and N2:Ar methods for measuring sediment denitrification—assumptions, modifications, and implications. Estuaries 25(6A):1077–1087. doi:10.1007/BF02692205

Faulkner SP, Patrick WH (1992) Redox processes and diagnostic wetland soil indicators in bottomland hardwood forest. Soil Sci Soc Am J 56:856–865

Fear JM, Thompson SP, Gallo TE, Paerl HW (2005) Denitrification rates measured along a salinity gradient in the eutrophic Neuse River Estuary, North Carolina, USA. Estuaries 28(4):608–619. doi:10.1007/BF02696071

Forshay KJ, Stanley EH (2005) Rapid nitrate loss and denitrification in a temperate river floodplain. Biogeochemistry 75:43–64. doi:10.1007/s10533-004-6016-4

Garcia-Ruiz R, Pattinson SN, Whitton BA (1998) Kinetic parameters of denitrification in a river continuum. Appl Environ Microbiol 64:2533–2538

Green PA, Vörösmarty CJ, Meybeck M, Galloway JN, Peterson BJ, Boyer EW (2004) Pre-industrial and contemporary fluxes of nitrogen through rivers: a global assessment based on typology. Biogeochemistry 68:71–105. doi:10.1023/B:BIOG.0000025742.82155.92

Gribsholt B, Boschker HTS, Struyf E, Andersson M, Tramper A, De Brabandere L, van Damme S, Brion N, Meire P, Dehairs F, Middleburg JJ, Heip CHR (2005) Nitrogen processing in a tidal freshwater marsh: a whole-ecosystem 15 N labeling study. Limnol Oceanogr 50(6):1945–1959

Gribsholt B, Struyf E, Tramper A, Andersson MGI, Brion N, De Brabandere L, van Damme S, Meire P, Middelburg JJ, Dehairs F, Boschker HTS (2006) Ammonium transformation in a nitrogen-rich tidal freshwater marsh. Biogeochemistry 80:289–298. doi:10.1007/s10533-006-9024-8

Gribsholt B, Struyf E, Tramper A, De Brabandere L, Brion N, van Damme S, Meire P, Dehairs F, Middelburg JJ, Boschker HTS (2007) Nitrogen assimilation and short term retention in a nutrient-rich tidal freshwater marsh—a whole ecosystem 15 N enrichment study. Biogeosciences 4(11):11–26

Groffman PM, Altabet MA, Bohlke JK, Butterback-Bahl K, David MB, Firestone MK, Giblin AE, Kana TM, Nielsen LP, Voytek MA (2006) Methods for measuring denitrification: diverse approaches to a difficult problem. Ecol Appl 16:2091–2122. doi:10.1890/1051-0761(2006)016[2091:MFMDDA]2.0.CO;2

Kana T, Weiss DL (2004) Comment on "comparison of isotope pairing and N2:Ar methods for measuring sediment denitrification" by BD Eyre, S Rysgaard, T Dalsgaard, and PB Christensen (2002) Estuaries 25:1077–1087. Estuaries 27:173–176. doi:10.1007/BF02803571

Kana T, Darkangelo C, Hunt D, Oldham J, Bennet G, Cornwell J (1994) Membrane inlet mass spectrometer for rapid high-precision determination of N_2, O_2, and Ar in environmental water samples. Anal Chem 66:4166–4170. doi:10.1021/ac00095a009

Kerner M, Kausch H, Miehlich G (1990) The effect of tidal action on the transformations of nitrogen in freshwater tidal flat sediments. Arch Hydrobiol Suppl 75:251–271

Leopold LB, Wolman MG, Miller JP (1964) Fluvial processes in geomorphology. WH Freeman, San Francisco

Lide (2004) Handbook of chemistry and physics. CRC, Boca Raton

Lindau CW, DeLaune RD, Pardue JH (1994) Inorganic nitrogen processing and assimilation in a forested wetland. Hydrobiologia 277:171–178

Machefert SE, Dise NB (2004) Hydrological controls on denitrification in riparian ecosystems. Hydrol Earth Syst Sci 8:686–694

McCarthy MJ, Lavrentyev PJ, Yang L, Zhang L, Chen Y, Qin B, Gardner WS (2007) Nitrogen dynamics and microbial food web structure during a summer cyanobacterial bloom in a subtropical, shallow, well-mixed, eutrophic lake (Lake Taihu, China). Hydrobiologia 581:195–207. doi:10.1007/s10750-006-0496-2

Mulholland PJ et al (2008) Stream denitrification across biomes and its response to anthropogenic nitrate loading. Nature 452:202–206. doi:10.1038/nature06686

Neubauer SC, Anderson IC, Neikirk BB (2005) Nitrogen cycling and ecosystem exchanges in a Virginia tidal freshwater marsh. Estuaries 28(6):909–922. doi:10.1007/BF02696019

Orr CH, Stanley EH, Wilson KA, Finlay JC (2007) Effects of restoration and reflooding on soil denitrification in a leveed Midwestern floodplain. Ecol Appl 17(8):2365–2376. doi:10.1890/06-2113.1

Phillips JD (1997) A short history of a flat place: three centuries of geomorphic change in the Croatan National Forest. Ann Assoc Am Geogr 87(2):197–216. doi:10.1111/0004-5608.872050

Pinay G, Ruffinoni C, Fabre A (1995) Nitrogen cycling in two riparian forest soils under different geomorphic conditions. Biogeochemistry 30:9–29. doi:10.1007/BF02181038

Pinay G, Black VJ, Planty-Tabacchi AM, Gumiero B, DéCamps H (2000) Geomorphic control of denitrification in large floodplain soils. Biogeochemistry 50:163–182. doi:10.1023/A:1006317004639

Pinay G, Gumiero B, Tabacchi E, Gimenez O, Tabacchi-Planty AM, Hefting MM, Burt TP, Black VA, Nilsson C, Iordache V, Bureau F, Vought L, Petts GE, DéCamps H (2007) Patterns of denitrification rates in European alluvial soils under various hydrological regimes. Freshw Biol 52:252–266. doi:10.1111/j.1365-2427.2006.01680.x

Schuchardt B, Haesloop U, Schirmer M (1993) The tidal freshwater reach of the Weser Estuary: riverine or estuarine? Neth J Aquat Ecol 27:215–226. doi:10.1007/BF02334785

Seitzinger S, Harrison JA, Bohlke JK, Bouwman AF, Lowrance R, Peterson B, Tobias C, Van Drecht G (2006) Denitrification across landscapes and waterscapes: a synthesis. Ecol Appl 16:2064–2090. doi:10.1890/1051-0761(2006)016[2064:DALAWA]2.0.CO;2

Seybold CA, Mersie W, Huang JY, McNamee C (2002) Soil oxidation-reduction potential, pH, temperature, and water-table patterns of a freshwater tidal wetland. Wetlands 22:149–158. doi:10.1672/0277-5212(2002)022[0149:SRPTAW]2.0.CO;2

Smith VH, Tilman GD, Nekola JC (1999) Eutrophication: impacts of excess nutient inputs on freshwater, marine, and terrestrial ecosystems. Environ Pollut 100:179–196. doi:10.1016/S0269-7491(99)00091-3

Tockner K, Pennetzdofer D, Reiner N, Schiemer F, Ward JV (1999) Hydrological connectivity, and the exchange of organic matter and nutrients in a dynamic river-floodplain system (Danube, Austria). Freshw Biol 41:521–535. doi:10.1046/j.1365-2427.1999.00399.x

Valett HM, Baker MA, Morrice JA, Crawford CS, Molles MC, Dahm CN, Moyer DL, Thibault JR, Ellis LM (2005) Biogeochemical and metabolic responses to the flood pulse in a semiarid floodplain. Ecology 86(1):220–234. doi:10.1890/03-4091

van Bochove E, Beauchemin S, Theriault G (2002) Continuous multiple measurement of soil oxidation-reduction potential using platinum microelectrodes. Soil Sci Soc Am J 66:1813–1820

Verhoeven JTA, Whigham DF, van Logtestijn R, O'Neill J (2001) A comparitive study of nitrogen and phosphorus cycling in tidal and non-tidal riverine wetlands. Wetlands 2:210–222. doi:10.1672/0277-5212(2001)021[0210:ACSONA]2.0.CO;2

Vitousek PM, Aber JD, Howarth RW, Likens GE, Matson PA, Schindler DW, Schlesinger WH, Tilman DG (1997) Human alteration of the global nitrogen cycle: sources and consequences. Ecol Appl 7(3):737–750

Wollheim WM, Vörösmarty CJ, Peterson BJ, Seitzinger SP, Hopkinson CS (2006) Relationship between river size and nutrient removal. Geophys Res Lett. doi:10.1029/2006GL025845

Wollheim WM, Vörösmarty CJ, Bouwman AF, Green P, Harrison J, Linder E, Peterson BJ, Seitzinger SP, Syvitski JPM (2008) Global N removal by freshwater aquatic systems using a spatially distributed, within-basin approach. Global Biogeochem Cycles. doi:10.1029/2007GB002963